









RESEARCH ARTICLE

10.1029/2023SW003731

Sudden Commencements and Geomagnetically Induced Currents in New Zealand: Correlations and Dependence

A. W. Smith¹ , C. J. Rodger² , D. H. Mac Manus² , I. J. Rae¹ , A. R. Fogg³ , C. Forsyth⁴ , P. Fisher², T. Petersen⁵ , and M. Dalzell⁶ 

¹Department of Mathematics, Physics and Electrical Engineering, Northumbria University, Newcastle upon Tyne, UK, ²Department of Physics, University of Otago, Dunedin, New Zealand, ³School of Cosmic Physics, DIAS Dunsink Observatory, Dublin Institute for Advanced Studies, Dublin, Ireland, ⁴Mullard Space Science Laboratory, UCL, Dorking, UK, ⁵GNS Science, Wellington, New Zealand, ⁶Transpower New Zealand Limited, Wellington, New Zealand

Key Points:

- The maximum H' and Geomagnetically Induced Current (GIC) observed during Sudden Commencements (SCs) correlates well ($r^2 \sim 0.7$) across New Zealand
- SCs that occur when New Zealand is on the dayside of the Earth are associated with 27% greater GICs for the same H' on average
- Extrapolation suggests that a hypothetical extreme SC (4000 nT min⁻¹) would be related to GICs over 2000 A near Dunedin

Correspondence to:

A. W. Smith,
andy.w.smith@northumbria.ac.uk

Citation:

Smith, A. W., Rodger, C. J., Mac Manus, D. H., Rae, I. J., Fogg, A. R., Forsyth, C., et al. (2024). Sudden commencements and geomagnetically induced currents in New Zealand: Correlations and dependence. *Space Weather*, 22, e2023SW003731. <https://doi.org/10.1029/2023SW003731>

Received 20 SEP 2023
Accepted 27 NOV 2023

Abstract Changes in the Earth's geomagnetic field induce geoelectric fields in the solid Earth. These electric fields drive Geomagnetically Induced Currents (GICs) in grounded, conducting infrastructure. These GICs can damage or degrade equipment if they are sufficiently intense—understanding and forecasting them is of critical importance. One of the key magnetospheric phenomena are Sudden Commencements (SCs). To examine the potential impact of SCs we evaluate the correlation between the measured maximum GICs and rate of change of the magnetic field (H') in 75 power grid transformers across New Zealand between 2001 and 2020. The maximum observed H' and GIC correlate well, with correlation coefficients (r^2) around 0.7. We investigate the gradient of the relationship between H' and GIC, finding a hot spot close to Dunedin: where a given H' will drive the largest relative current (0.5 A nT⁻¹ min). We observe strong intralocation variability, with the gradients varying by a factor of two or more at adjacent transformers. We find that GICs are (on average) greater if they are related to: (a) Storm Sudden Commencements (SSCs; 27% larger than Sudden Impulses, SIs); (b) SCs while New Zealand is on the dayside of the Earth (27% larger than the nightside); and (c) SCs with a predominantly East-West magnetic field change (14% larger than North-South equivalents). These results are attributed to the geology of New Zealand and the geometry of the power network. We extrapolate to find that transformers near Dunedin would see 2000 A or more during a theoretical extreme SC ($H' = 4000$ nT min⁻¹).

Plain Language Summary A changing magnetic field at the surface of the Earth will induce anomalous currents in conducting infrastructure, such as a power network. There are many processes that can cause the Earth's magnetic field to change, but we investigate one of the simplest: Sudden Commencements (SCs). SCs are caused by rapid increases in the density or velocity of the solar wind, and can be measured as a fast, mostly Northward change of the magnetic field on the ground. We compare the changes in the magnetic field with the currents observed at 75 locations across the New Zealand power network. We find a link between the changes in the magnetic field and the currents, but several locations appear to be more susceptible to large currents. We also find that some types of SC appear to cause larger currents and that the effect of SCs is greater on the sunlit side of the Earth. Finally, we use the relationships we have seen over the last 20 years to see what would happen if a much larger event were to occur in the future.

1. Introduction

The interaction between the solar wind and the Earth's magnetic field results in a large range of magnetospheric processes. Many of these global magnetospheric phenomena change the Earth's magnetic field and generate dynamic currents in the ionosphere. Consequently, a large range of magnetospheric processes are linked to rapid changes in the measured magnetic field on the surface of the Earth. This changing magnetic field - through Faraday's law - will induce an electric field in the solid Earth, which will in turn generate anomalous currents in grounded conducting infrastructure, known as Geomagnetically Induced Currents (GICs). Presenting as an induced direct current (DC), these GICs can cause the immediate failure of components in power infrastructure, in addition to prematurely aging equipment (Beland & Small, 2004; Bolduc, 2002; Boteler et al., 1998; Gaunt & Coetzee, 2007; Rajput et al., 2020). It has been estimated that an extreme space weather event, and corresponding large GICs, would result in the loss of billions of dollars for a western economy (Eastwood et al., 2018), including

© 2024. The Authors.

This is an open access article under the terms of the [Creative Commons Attribution License](https://creativecommons.org/licenses/by/4.0/), which permits use, distribution and reproduction in any medium, provided the original work is properly cited.

around £16 billion for the UK alone (Oughton et al., 2019). We therefore need to better understand and predict such events, enabling cost-saving mitigation to be undertaken.

The magnitude of GICs that will be generated depends on several key factors, including: the orientation and frequency content of the changing magnetic field (Clilverd et al., 2020; Heyns et al., 2021; Smith et al., 2022); the conductivity profile of the local region (Bedrosian & Love, 2015; Beggan, 2015; Cordell et al., 2021; Dimmock et al., 2019, 2020); and the details of the geometry and electrical properties of the conducting infrastructure (Beggan et al., 2013; Blake et al., 2018; Divett et al., 2018, 2020; Mac Manus, Rodger, Dalzell, et al., 2022). However, in general it has often been assumed that a larger rate of change of the magnetic field will drive larger GICs (Mac Manus et al., 2017; Smith et al., 2022; Viljanen et al., 2001). For this reason, much recent effort has been made to forecast the rate of change of the magnetic field (e.g., Blandin et al., 2022; Keesee et al., 2020; Madsen et al., 2022; Pinto et al., 2022; Upendran et al., 2022; Wintoft et al., 2015), or the probability that it will exceed defined thresholds (e.g., Camporeale et al., 2020; Coughlan et al., 2023; Pulkkinen et al., 2013; Smith, Forsyth, Rae, Garton, et al., 2021). The focus on the magnetic field, rather than GICs, has partly been necessitated by the typical scarcity of freely available GIC observations, compared to the relative abundance of magnetic field measurements.

Historically, GICs have been inferred to cause damage to power systems: for example, in Quebec, Canada in 1989 (Beland & Small, 2004; Bolduc, 2002), Dunedin, New Zealand in 2001 (Rodger et al., 2017) and Malmö, Sweden in 2003 (Pulkkinen et al., 2005). For the incidents in Dunedin and Malmö, the first reported failures of electrical equipment were associated with the Sudden Commencement (SC) which preceded the start of a period of intense geomagnetic disturbance: a geomagnetic storm (Pulkkinen et al., 2005; Rodger et al., 2017). An SC is a rapid change in the Earth's magnetic field (Araki, 1994; Fiori et al., 2014), related to the impact of an increase in solar wind dynamic pressure, often a shock or discontinuity on near-Earth space (Lühr et al., 2009; Oliveira et al., 2018; Smith et al., 2020; Takeuchi et al., 2002). These shocks often precede other structures in the solar wind, such as CMEs (Coronal Mass Ejections) that are known to further drive elevated levels of magnetospheric activity (Akasofu & Chao, 1980; Gonzalez et al., 1994; Yue et al., 2010; Zhou & Tsurutani, 2001), and consequently ground magnetic field variability and related GICs (e.g., Dimmock et al., 2019; Love et al., 2022; Mac Manus, Rodger, Ingham, et al., 2022; Rogers et al., 2020; Smith et al., 2019; Smith, Forsyth, Rae, Rodger, & Freeman, 2021). SCs are often subdivided into two broad categories: those that are followed by further magnetospheric activity, termed Storm Sudden Commencements (SSCs); and those that are not, which are termed Sudden Impulses (SIs) (e.g., Mayaud, 1973).

Amongst the key magnetospheric drivers of large changes of the geomagnetic field, SCs are one of the most simple to model. However, while often considered as simply northward deflections of the magnetic field, the magnetic field signature has two main components, whose relative dominance varies with latitude: the DL and DP perturbations (Araki, 1994). The DL component—dominant at low latitudes—is the direct compressional contribution, driven by the inward motion of the magnetopause and necessarily increased magnetopause current. Meanwhile, the DP component—dominant at high latitudes—is caused by the compressional wave (launched by the inward magnetopause motion) coupling to shear Alfvén waves in the magnetosphere (Southwood & Kivelson, 1990), the ionospheric footprints of which are linked to twin traveling convection vortices (TCVs) in the high latitude ionosphere (Friis-Christensen et al., 1988). These vortices move away from the noon meridian, but their strength maximizes around 0900 solar local time (Moretto et al., 1997). Therefore, the ground magnetic field signature and the “size” of an SC on the ground will vary with both latitude (e.g., Fiori et al., 2014; Fogg, Lester, et al., 2023; Smith, Forsyth, Rae, Rodger, & Freeman, 2021; Takeuchi et al., 2002) and local time (e.g., Kokubun, 1983; Russell et al., 1992).

While SCs represent a relatively simple signature, there is inherent variability in the frequency content and the vector rate of change of the magnetic field during an SC (e.g., with MLT) which provides a source of uncertainty to simple mappings between the observed magnetic field changes and GICs, even at a fixed location. Examining more than 15 years of GIC observations made at a single power grid transformer near Christchurch in New Zealand, Smith et al. (2022) showed that SCs that occurred while New Zealand was on the dayside of the planet were related to GICs that were 30% larger than if New Zealand were on the night-side for the same magnetic field rate of change. This could not be accounted for by controlling for the dominant orientation of the largest rate of change of the field, and was inferred to be partly due to the different frequency content of the SC signature at different local times.

In this study, we expand on the work of Smith et al. (2022), assessing how GIC observed at 75 different power grid transformers in the New Zealand power network are impacted by SCs. We determine whether the type of SC

is important, if the previous day/night asymmetry is common across the network, and how the dominant orientation of the SC signature impacts distinct part of the system. Finally, we assess the GICs that would be induced during a reasonable, but extreme geomagnetic disturbance occurring at a mid latitude location (e.g., New Zealand or indeed the United Kingdom/Ireland).

2. Data

In this study we utilize the long-term magnetic field observations made at the Eyrewell (EYR) magnetometer station, at a cadence of 1 min. In particular, we calculate the rate of change of the horizontal component of the magnetic field (H'), which been shown in the past to correlate well with observed GICs (e.g., Mac Manus et al., 2017; Smith et al., 2022; Viljanen et al., 2001).

We compare these magnetic field observations with GIC data from 22 substations around New Zealand, at which we have data from 75 different transformers (in many substations there are multiple transformers which are instrumented to measure GIC). GIC data from these transformers have been collected for different lengths of time, but overall we investigate the period between 2001 and 2020. A detailed description of the instrumentation and method by which the GIC data have been generated can be found in Mac Manus et al. (2017). Further, Clilverd et al. (2020) describe how the data are recorded at 4 s resolution if the GICs observed are dynamic, as would be expected during an SC. The time resolution is lower if the GIC values are changing little (e.g., less than 0.2 A). For this study, we use uncompressed 4 s data.

To identify Sudden Commencements, we initially use the SOHO interplanetary shock list. This catalog has been derived through the use of the ShockSpotter method (<https://space.umd.edu/pm/>) on data from the SOHO spacecraft at the L1 point. The SOHO list has then been inspected to ensure that there is a clear and recognizable SC signature (i.e., a magnetic field deflection close to the predicted shock impact time) seen in the magnetometer data recorded at EYR. For the period between 2001 and 2020 this list comprises a total of 232 SCs, a subset of which will have the requisite GIC data at each of the 75 transformers. Further, we define an SSC to be an SC that is followed within 24 hr by a SymH of -50 nT or less, a similar criteria to that typically employed (e.g., Fiori et al., 2014; Fogg, Jackman, Coco, et al., 2023; Smith, Forsyth, Rae, Rodger, & Freeman, 2021). Meanwhile, if SymH exceeds -50 nT for the 24 hr after the SC then it is categorized as an SI.

2.1. Method

In this study we investigate the correlation between the maximum rate of change of the horizontal magnetic field (H') and the GICs observed in 75 transformers across 22 substations in New Zealand. We expand the work of Smith et al. (2022), who investigated this relationship for a single transformer in Christchurch (ISL M6, i.e., transformer number 6 from the Islington substation). For both H' and the GIC observations we take the maximum value observed from -30 s before the impact of the SC to 150 s afterward, in order to account for time aliasing and inductance within the power system, following the same process as in Smith et al. (2022). The gradient of the correlation provides an indication of the susceptibility of the transformer to GICs, effectively how easily a given rate of change of the magnetic field (H') will drive GICs for a transformer in that part of the network.

Figure 1 shows the correlation between the maximum H' and GIC observed at four example transformers. The correlations have been fit using linear orthogonal distance regression (ODR), as it allows consideration that both variables may have uncertainty (in contrast to ordinary least squares). The fit parameters and uncertainties are provided on the panels, along with the r^2 of the correlations. The fits are constrained to lie through the origin (i.e., a linear fit with zero constant), though we note that this largely does not change the fits obtained. These four transformers have been selected on the basis that their correlations provide a range of gradients, from 0.021 A nT^{-1} min at the WTK (Waitaki) transformer to 0.598 A nT^{-1} min at the HWB (Halfway Bush, Dunedin) transformer. For comparison we have also included ISL M6 (Islington), which formed the basis of a previous study (Smith et al., 2022). ISL M6 was selected previously as it provides the longest continuous GIC measurements - as seen from the 183 SCs from which we have data.

While a range of gradients are observed in the four example transformers, we note that the correlations are high - with r^2 values above 0.75. However, there is some scatter evident in Figure 1, particularly in the lower two panels where the gradients of the correlations are higher. At ISL M6 (Figure 1b) this scatter has been linked to the more precise detail of the SC magnetic signature, such as the directionality and frequency content of the magnetic changes (Smith et al., 2022).

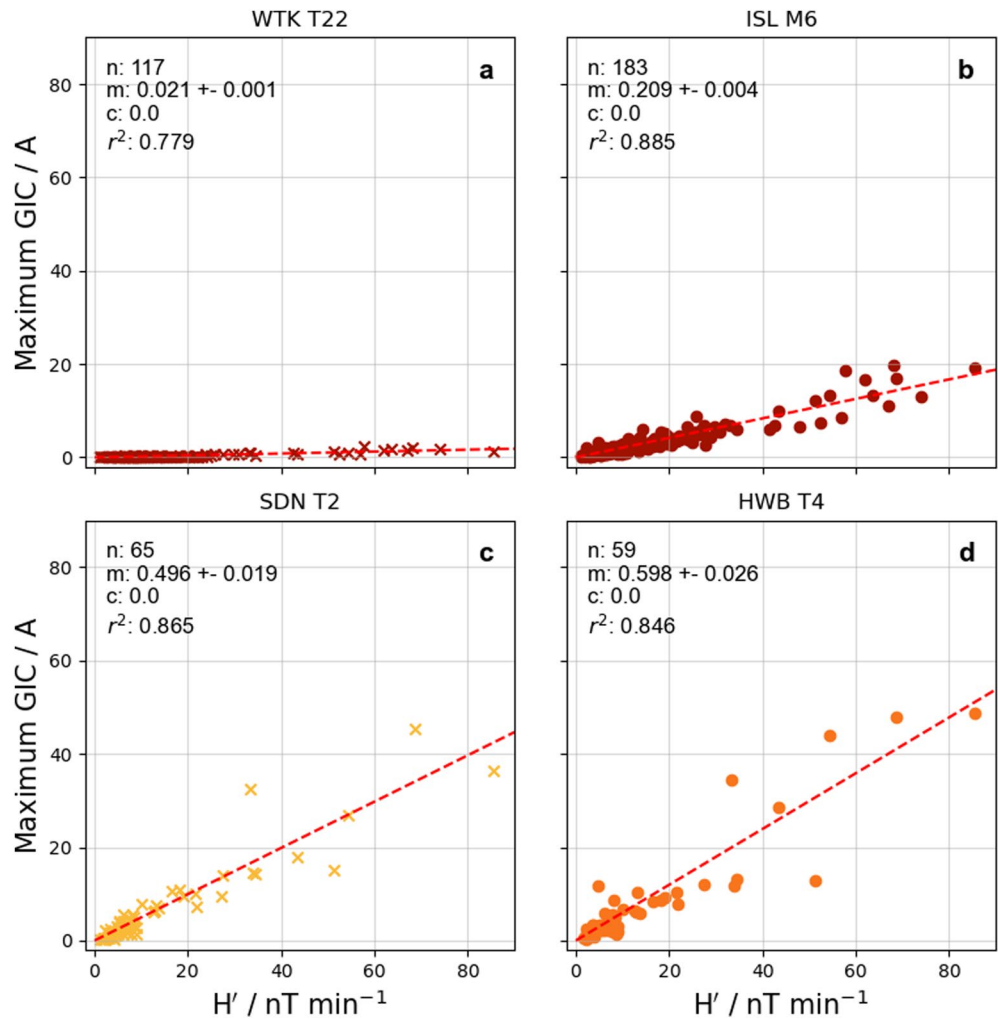


Figure 1. The correlations between the maximum H' and GIC observed during Sudden Commencements (SCs) at four example transformers: (a) Waitaki number 22, (b) Islington number 6, (c) South Dunedin number 2, and (d) Halfway Bush number 4. Linear fits and the fit parameters obtained through orthogonal distance regression are included for each transformer.

For context, an observed GIC of 5 A has been inferred to be “significant” for some types of transformer that are present in the New Zealand power network (Mac Manus et al., 2017), with large geomagnetic storms being associated with GICs of between 20 and 50 A. The transformer failure at HWB in Dunedin in 2001 has been linked to GICs of around 100 A (Rodger et al., 2017), though indications of transformers being under considerable stress have been observed at much lower levels of GIC (Rodger et al., 2020). We can see in Figure 1 that all of the observed GICs during SCs at the four example stations are below ~50 A in the period of study.

3. Results

In Figure 2a, we show the gradients that are obtained at the 75 transformers across New Zealand, with associated uncertainties, ordered alphabetically. The lower panel, Figure 2b, provides contextual information with the points showing the r^2 associated with the correlations (left axis), and the bars showing the number of SCs for which there was sufficient GIC and magnetometer data (right axis). Transformers with fewer than five SCs, or with an r^2 less than 0.5 are indicated with a gray cross (+) in Figure 2a—totaling 21 of the 75 transformers.

Previously, Smith et al. (2022) investigated ISL M6, finding a gradient of 0.21 A $\text{nT}^{-1} \text{min}$. While ISL M6 was selected as it had the longest historical data set—equivalent to the largest number of SCs in the sample period (Figure 2b)—we can see that the gradient of the correlation at ISL M6 is by no means anomalous. Three transformers at two locations show gradients over a factor of two larger (0.5 A $\text{nT}^{-1} \text{min}$ and above): Halfway Bush

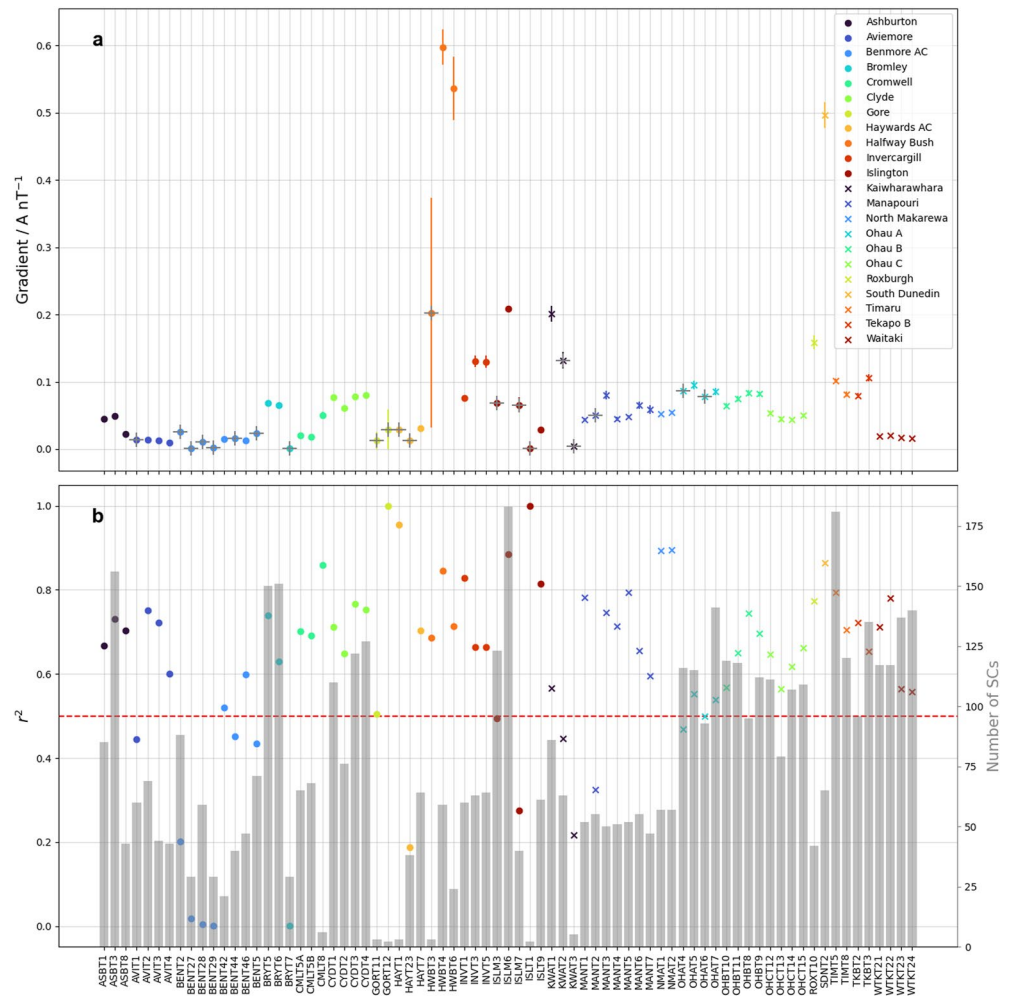


Figure 2. A statistical summary of the correlations between the maximum observed H' and GICs at the 75 transformers (22 substations) in our study. Top, (a) the gradient associated with the correlation (with uncertainty represented by the standard deviation), with the color/marker indicating the geographical location (i.e., substation). Bottom, (b) contextual information regarding the r^2 (points, left axis) and number of events (bars, right axis) for each transformer. The horizontal red dashed line indicates an r^2 of 0.5. Transformers with fewer than five SCs, or with an $r^2 < 0.5$ are indicated in panel (a) with a gray cross (+).

(HWB) and South Dunedin (SDN). However, we see that at the vast majority of locations the gradients are much lower, less than $0.1 \text{ A nT}^{-1} \text{ min}$. This speaks to a large difference in the GIC experienced across New Zealand during SCs, and the complex interplay between the geology of the country and the distribution and design of the power network. Interestingly, we also see significant variability between different transformers within the same location, likely due to different earthing or winding resistances. For example, at Ashburton (black dots) and Invercargill (red dots) we see differences of around a factor of two between different transformers. This is consistent with what has been reported before in the New Zealand data, with large differences between closely spaced substations (e.g., Mac Manus et al., 2017, Figure 5) and inside the same substation (Divett et al. (2018), Table 1).

3.1. Geographical Distribution

Figure 3a shows the geographical distributions of the gradients reported in Figure 2, focused on the South Island and lower North Island of New Zealand. A northward offset is used to separate any transformers at the same location, while any transformers with a correlation below 0.5, or fewer than five SCs in the data set, are colored gray. As above, we see across most of New Zealand the gradients obtained are around $0.1 \text{ A nT}^{-1} \text{ min}$, however Dunedin and Halfway Bush (colored yellow in the lower South East) are a very clear exception. Further north,

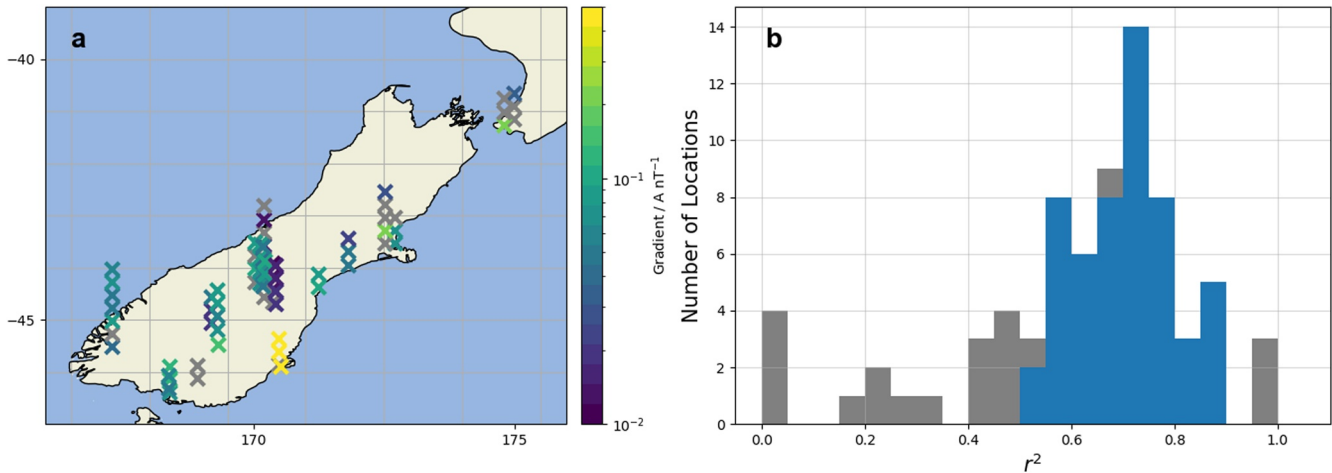


Figure 3. The gradient of the correlation between the maximum H' and GIC observed during SCs. Left, (a) the distribution of the transformers across New Zealand. Where multiple transformers are found at the same geographical location a northward offset is added to separate the observations visually. Right, (b) a stacked histogram of the r^2 obtained from the correlations. Transformers where less than five SCs were recorded, or an r^2 below 0.5 was obtained, are included in gray.

around the Christchurch peninsula ($\sim 173^\circ$ longitude, -44° latitude) we see another region of moderately higher gradient. We note that this is close to the Eyrewell magnetometer, whose data are used for the correlations. We will discuss the use of the single magnetometer station in Section 4.1. The noted intra-location variability is also clear from Figure 3, particularly in the densely sampled region in the center of the South island.

3.2. Geomagnetic Storm Relation

Recently, Smith et al. (2022) found that ISL M6 observed a 22% greater GIC if the SC was followed by a geomagnetic storm (an SSC), as opposed to an isolated SC (an SI). In this work, we test if the difference between SSC and SIs holds across the New Zealand network. Figure 4 shows a comparison between the gradients of the correlation (between the maximum H' and GIC) obtained for SSCs and SIs. If these gradients are the same, then the points would lie along the black dashed line of gradient unity in Figure 4a, and the ratio in Figure 4b would be equal to one. Transformers for which there were data for fewer than five SSCs and SIs or an r^2 lower than 0.5 was recovered are colored gray.

There is considerable scatter at low gradients in Figure 4, however a large portion of the scatter is contributed by events for which there are few SSCs/SIs or poor correlations (i.e., in gray). Limiting our analysis to the 27 transformers with sufficient data and clear correlations (i.e., the non-gray points in Figures 4a and 4b), shows a clear preference for larger gradients during SSC-type events. The ratio of the gradients observed for SSC-related events to SI-related events is shown in Figure 4b. The mean of the 27 transformers with sufficient data shows that SSCs drive 26% greater GICs for a given H' , and therefore the results from ISL M6 are representative of those in the wider network. Some transformers show a difference of up to 40% between SSCs and SIs, indicating a systematic uncertainty associated with connecting a given H' to a GIC.

3.3. Local Time and Directional Dependence

Smith et al. (2022) also showed that the gradient between H' at EYR and the GIC amplitude at ISL M6 varied depending on two other factors. The first is that SCs that occur when New Zealand is on the dayside of the planet appear 30% more efficient at generating GICs for the same H' , while the second is that SCs whose magnetic signature was predominantly in the East-West direction are linked to 36% larger GICs. Figure 5 explores whether these key relations hold for other locations, in a similar format to Figure 4. Once more, subsets of events for which there are fewer than 5 events or with correlations (r^2) below 0.5 are shown in gray in Figures 5a and 5b, and are not included in the histograms in Figures 5c and 5d.

Figure 5a shows the comparison between those SCs that occur when New Zealand is on the dayside and nightside of the Earth. In total, 49 out of 75 transformers have sufficient data and high enough correlations to be included

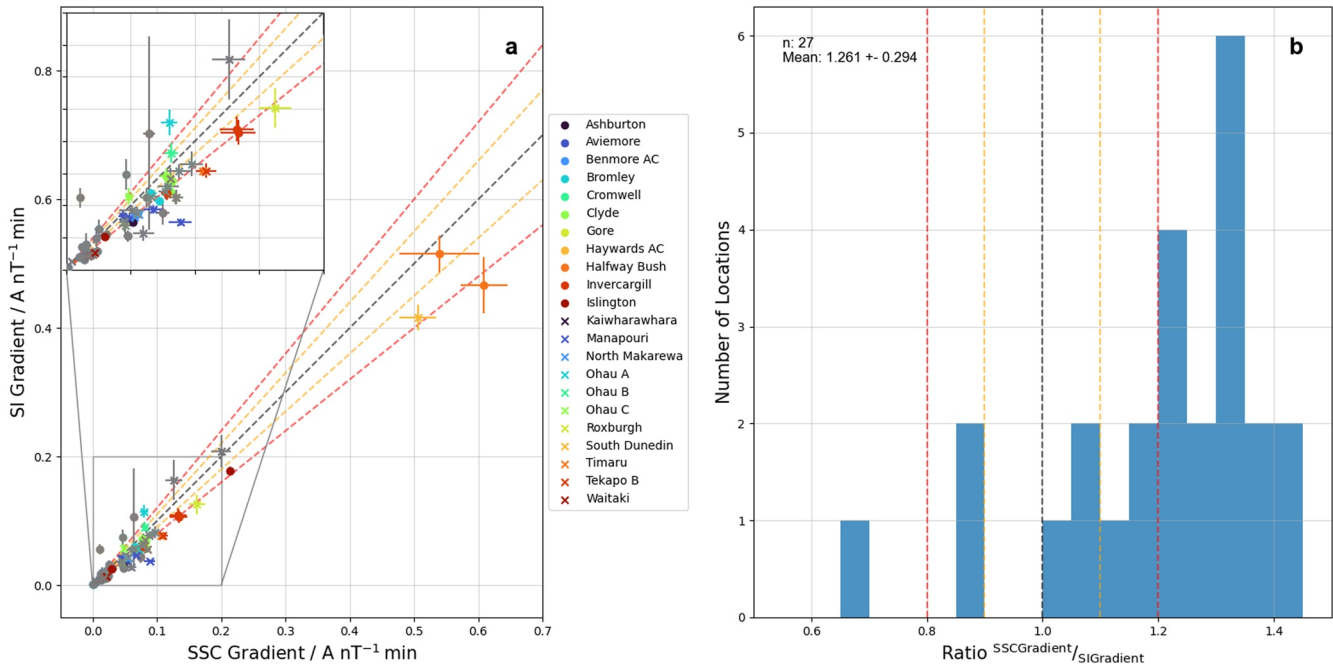


Figure 4. A comparison of the gradients of the correlations (between the maximum H' and GIC) obtained during SSC-type and SI-type events. Left, (a) a direct comparison of the gradients at each of the 75 locations. Right, (b) a histogram of the ratio of the gradients. For both panels the yellow and red dashed lines indicate differences of 10% and 20%, respectively. Locations for which there are fewer than five events in either category, or an r^2 of less than 0.5 is recovered, are indicated in gray, and are not included in histogram.

in this analysis and comparison. There appears to be a shift, particularly at smaller gradients (e.g., less than 0.3 A nT⁻¹ min), with the “day” gradients being larger by 20% or more. However, this difference is smaller for the three transformers with larger gradients (located at South Dunedin and Halfway Bush). Nonetheless, inspecting the ratios in Figure 5c, we see that on average the gradients are 27% larger when New Zealand is on the dayside of the Earth, and they can be over 40% larger at some locations.

Further, in Figure 5b we see that below 0.3 A nT⁻¹ min SCs whose largest rate of change is predominantly in the east-west direction (“dY” events) are linked to peak GICs that are over 10% greater. However, once more any difference is weaker or non-existent ($\sim\pm 10\%$) for those transformers with larger gradients (>0.3 A nT⁻¹ min). Inspecting the ratios in Figure 5d we see that the distribution is indeed skewed, with dY dominant events more often being linked to larger gradients.

While the mean of both ratios is skewed toward dayside and dY dominant events, there are transformers and locations where this is not the case. It is possible that there are geographical effects, with any effect occurring (or not occurring) in certain regions, given the geometry of the power network and geology of the local area.

Figure 6 explores the geographical distribution of the results in Figure 5. The top two rows show the gradients of the correlations obtained when New Zealand is on the day/night side (left) and for SCs for which the maximum rate of change is predominantly in the east/west direction (right). Figures 6e and 6f show the ratios of the gradients above: the geographical distribution of the data in Figures 5c and 5d. As before, if there are fewer than five SCs within each subset, or the correlation is low ($r^2 < 0.5$) then the points are colored gray. In the bottom of Figure 6 we limit the display to those events where the difference between the subsets are statistically significant at the $p = 0.05$ level.

In Figure 6e we see that most transformers are red in color, indicating that the gradients when New Zealand are on the dayside are greater (as discussed above). Interestingly, transformers for which this is not the case (i.e., blue crosses) are not limited to one location, but are in fact found at several locations in the South and West of the South Island - in places where adjacent transformers see stronger dayside gradients. We note that the majority of the data are retained from Figures 6e–6g, indicating that most of the day/night differences are statistically significant at the $p = 0.05$ level.

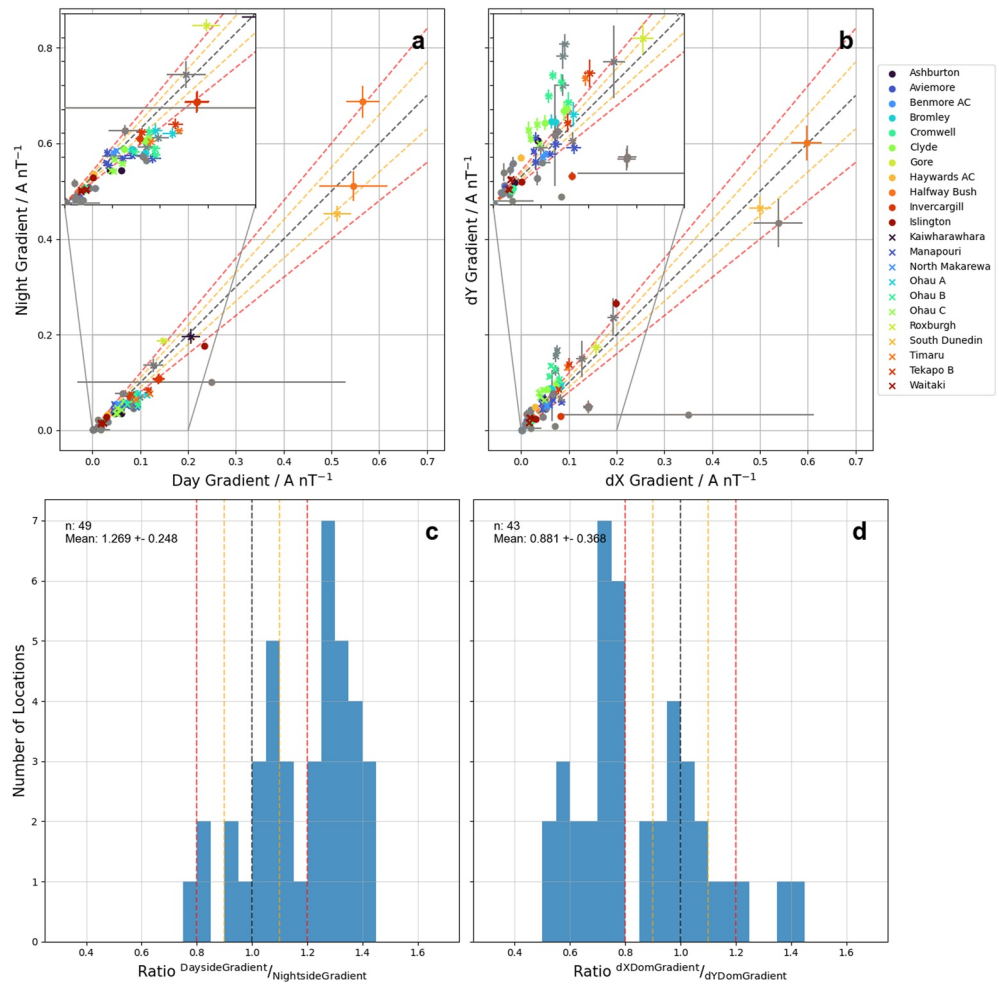


Figure 5. A comparison of the gradients of the correlations obtained for SCs when New Zealand is on the dayside/nightside of the Earth (a and c), and dX/dY dominant SCs (b and d), in a similar format to Figure 4.

Meanwhile, in Figure 6f, the majority of transformers are colored blue, this time showing that SCs that are predominantly in the east-west direction (dY dominant) are associated with a correlation with a steeper gradient. However, there are more transformers for which this is not the case as compared to Figure 6e. While these exceptions are mostly spread out across the South Island, they do appear more prevalent in the South and West: in particular the Southern-most locations are mostly characterized by North-South (dX) dominant SCs being linked to larger gradients.

4. Discussion

4.1. Spatial Variability of the Magnetic Field

Within the analysis above we have used the data from a single magnetic field observatory (Eyrewell, EYR), out of necessity. This single station has then been compared to the GICs recorded at 75 transformers (in 22 substations) across New Zealand. However in Europe, the rate of change of the magnetic field has been found to vary by factors of two to three over distances of ~500 km (Dimmock et al., 2020), albeit at a comparatively high latitude. More generally magnetic disturbances at mid-latitudes have been found to correlate well over a scale of several hundred kilometers (Dimitrakoudis et al., 2022). This may be a source of uncertainty in our study: the South Island is approximately 700 km in length. The source of the spatial variability of the magnetic field is both the small-scale size of the inducing ionospheric current systems (e.g., Forsyth et al., 2014; Ngwira et al., 2015, 2018; Pulkkinen et al., 2003) and complexity in the ground conductivity profiles (e.g., Bedrosian

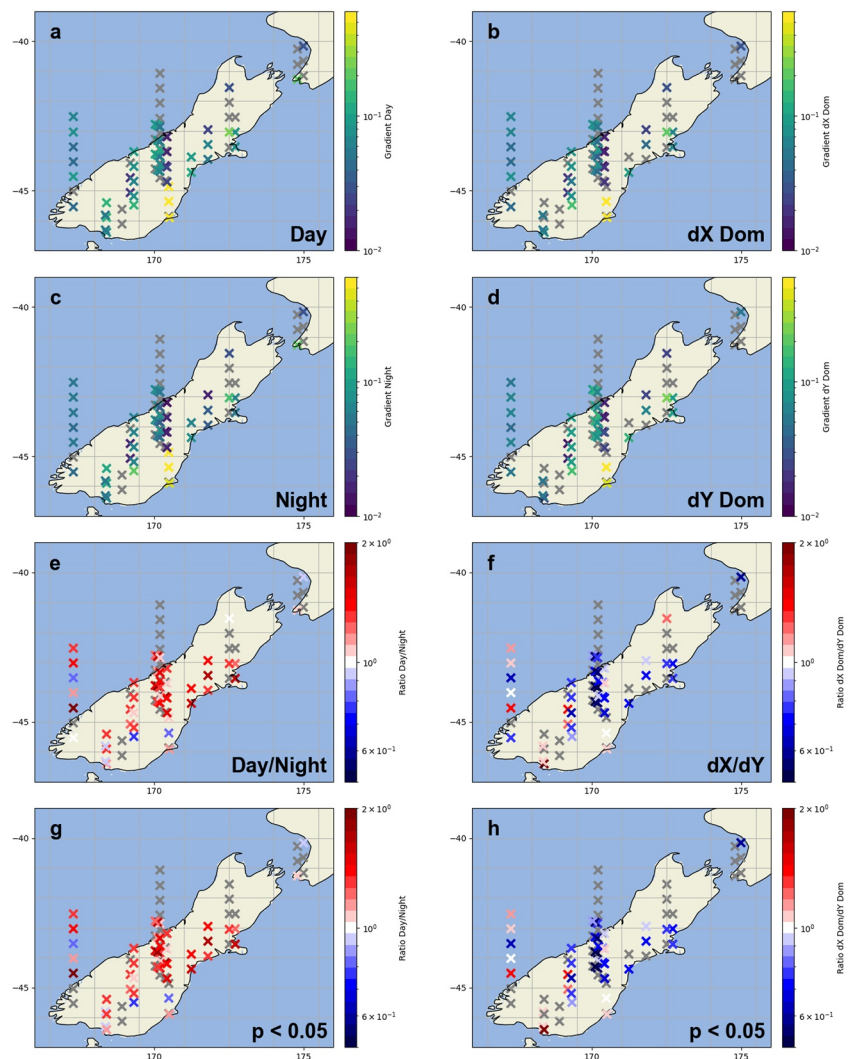


Figure 6. The geographical distribution of gradients in New Zealand, left: comparing dayside and nightside SCs; right: comparing the dX and dY dominant SCs. As in Figure 3, where multiple transformers are at a single location an additional northward offset is applied to separate the points. Left, (a, c, e, g): the gradient for dayside and nightside SCs (a, c), the ratio of dayside/nightside with all valid transformers (e), and only those with a statistically significant ($p < 0.05$) difference (g). Right, (b, d, f, h): the gradient for dX and dY dominant SCs (b, d), the ratio of dX/dY SCs with all valid transformers (f), and only those with a statistically significant ($p < 0.05$) difference (h). As above, if fewer than 5 SCs are available or a correlation (r^2) below 0.5 is obtained then the transformer is colored gray.

& Love, 2015; Beggan, 2015). Nevertheless, the currents associated with SCs are thought to be relatively large scale (Araki, 1994; Friis-Christensen et al., 1988; Kokubun, 1983; Russell et al., 1992), at least compared with those associated with substorms (e.g., Forsyth et al., 2014; Ngwira et al., 2018). Whilst the ground conductivity profiles are fixed at each measurement location, the consequences of the geology will depend upon the direction of the field changes, as well as their frequency content (e.g., Clilverd et al., 2020), both of which have been highlighted as important and variable for SCs (Smith et al., 2022). These factors will introduce intrinsic scatter in our correlations.

The use of the Eyrewell magnetometer will be most valid for the stations around the middle of the South Island, where the majority of data resides. We note that we do not see a strong relationship between the correlation (e.g., r^2) obtained comparing the maximum H' and GIC during SCs and the distance from the Eyrewell magnetometer, for example, in Figure 3. In fact, some of the poorest correlations are obtained at Islington, the most proximate location to the magnetometer site at Eyrewell. We find that the majority of transformers evaluated return an r^2 of around 0.7, which is comparable to that obtained in previous works for close magnetometers and GIC measurements (Smith et al., 2022).

4.2. Local Time and Vector Orientation Dependence

SCs are often observed in one minute resolution magnetic field data (e.g., Fiori et al., 2014; Oliveira et al., 2018; Smith et al., 2019; Smith, Forsyth, Rae, Rodger, & Freeman, 2021). Within these data sets, particularly when assessing the rate of change of the magnetic field or H' , SCs can appear to be a single family of magnetic signatures - a sharp spike that may last for several minutes. However, there is considerable structure to these magnetic field changes (e.g., Fogg, Lester, et al., 2023). An SC can be described by two separate components: the DL and DP components, or compressional and Alfvénic contributions as described above (Araki, 1994). The strength of these two components will determine the frequency content and orientation of the magnetic field signature, both of which depend on the location in latitude and local time.

A previous study of the link between SCs and GICs in New Zealand noted that the correspondence was dependent upon the local time and the dominant direction of the largest rate of change of the field (Smith et al., 2022). The local time dependence was inferred to be a result of a combination of the sub-minute resolution detail of the SC signature, and vector direction—both of which were inferred to be different on the dayside of the planet. Ultimately, SCs that were directed predominantly in the East-West direction, or were observed when New Zealand was on the dayside were associated with GICs at ISL M6 that were 36% and 30% larger, respectively.

In this work we confirm that, at least for the transformers in New Zealand for which we have sufficient data, the relationships earlier reported for ISL M6 predominantly hold true. On average, transformers observe 27% stronger GICs if New Zealand is on the dayside of the Earth, and 14% larger GICs if the largest H' is oriented mostly in the East-West direction. However, we do find some transformers for which this is not the case. These results demonstrate that the full vector, sub-minute resolution magnetic field signature is important to consider when interpreting the space weather impact of a given event. Much work in recent times has focused on forecasting the one minute rate of change of the geomagnetic field (e.g., Blandin et al., 2022; Keese et al., 2020; Pinto et al., 2022; Wintoft et al., 2015), or when it will exceed predefined thresholds (Camporeale et al., 2020; Coughlan et al., 2023; Pulkkinen et al., 2013; Smith, Forsyth, Rae, Garton, et al., 2021). However, we have shown that even if the magnitude of H' is predicted perfectly, and even though H' and GIC linearly correlate rather well (Mac Manus et al., 2017; Viljanen et al., 2001), any GIC derived through a simple correlation will still come with considerable uncertainty due to the orientation of H' and the sub-minute frequency content of the magnetic changes. We note that the differences derived above (i.e., 30% depending on local time and 14% depending on the orientation), are found for the horizontal ground magnetic field changes observed at ground level for a relatively simple magnetospheric process that can be described by a limited range of components: for more complex phenomena such as substorm current systems it is likely that there will be greater uncertainty in any linear mapping between GICs and H' .

4.3. Intra-Location Variability

We believe that one of the most interesting findings from the current study is the intra-location variability in the GICs recorded during SCs. In Figure 2 we can see that some locations (e.g., Ashburton, Cromwell, Invercargill and Islington) show differences of around a factor of two between transformers. As the magnetic field data (i.e., H') are fixed by the use of the EYR magnetic observatory, this intra-location variability must come from the GIC observations - assuming that approximately the same subset of SCs are being compared. Further, in Figure 6 we see that the transformers at a single location respond in different ways to the orientation of SCs: some will be more sensitive to North-South oriented SCs while others nearby will be related to larger GICs for East-West oriented SCs. This highlights the importance of the specific set up of each transformer, the connectivity and resistances for example, in determining the GIC that will flow, and the limitations of calculating a single GIC at each location. Transformer-level modeling of GICs is required (e.g., Divett et al., 2018; Mac Manus, Rodger, Ingham, et al., 2022).

4.4. Extreme Events

Large historical events are often scaled to estimate the impact of more extreme events. For example, Mac Manus, Rodger, Dalzell, et al. (2022) scale large events from the past 30 years such that the maximum value of H' matches those expected from the literature: in this case for a maximum value of 4000 nT min⁻¹. This value corresponds to the upper limit of the 95% confidence limit for a 100 years return period at New Zealand's geomagnetic latitude

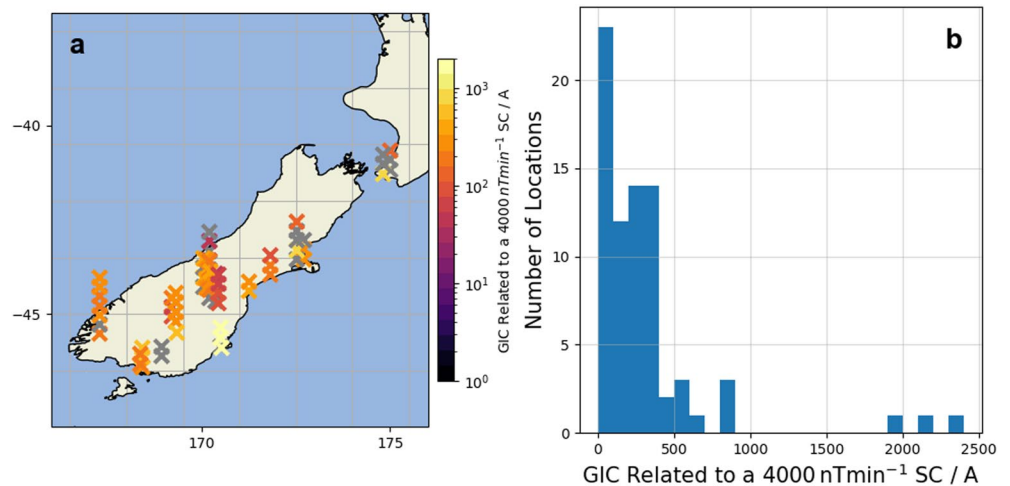


Figure 7. The GIC extrapolated to result from a H' of 4000 nT min^{-1} during an SC. Left (a), the geographical distribution of GIC, a northward offset has been added to additional transformers at the same location to improve the clarity. Right (b), the distribution of GIC observed.

(Thomson et al., 2011). It is also consistent with the 5000 nT min^{-1} reported by a recent worst-case-scenario report for comparable geomagnetic latitudes in the UK (Hapgood et al., 2021). We note that during the October 2003 and September 2017 geomagnetic storms the largest H' at EYR was observed during the SC at the start of the storm (Figure 1 of Mac Manus, Rodger, Dalzell, et al. (2022)).

Motivated by this, Figure 7 details the GICs that would be observed across New Zealand, should an SC-related H' of 4000 nT min^{-1} be recorded - assuming that the correlations reported above hold true. Most locations would incur a GIC of $<500 \text{ A}$. However, we see that South Dunedin is exposed to particularly large GICs of $\sim 2000 \text{ A}$, a finding that is consistent with Dunedin being the location where power infrastructure was impacted during an SC in the past (Rodger et al., 2017). These are extremely high levels, vastly beyond anything that has been recorded in the New Zealand network during our study interval, and well above that which would cause concern (Mac Manus, Rodger, Dalzell, et al., 2022). As discussed above, we also see large variations within locations - near Christchurch the inferred maximum GICs in different transformers span several orders of magnitude. We note that it is currently not known how an SC giving a H' of 4000 nT min^{-1} would correspond to a solar wind transient. The results of Fogg, Jackman, Malone-Leigh, et al. (2023) suggest that for a location in Ireland, at a similar magnetic latitude to EYR, the onset of an SC may contribute extreme H' , but processes during the main and recovery phases of geomagnetic storms have contributed larger extreme H' observations in the past. Indeed at mid-latitudes in Europe, the three days following an SSC have been found to contain the vast majority of extreme rates of change of the magnetic field (Smith et al., 2019; Smith, Forsyth, Rae, Rodger, & Freeman, 2021). This is a topic that should be further explored in the future.

5. Summary and Conclusions

In this work we have investigated the correlation between the largest H' and GIC recorded during Sudden Commencements (SCs) over the last 20 years across the New Zealand power network. We use data from 75 transformers, spanning 22 substations across the country, though mostly located in the South Island.

We find that for the majority of the 75 transformers the maximum H' and GIC during SCs correlates to a high degree, typically $r^2 \sim 0.7$. We then focus on the gradient of the correlation, effectively the magnitude of the GIC observed per unit H' . The gradient of the correlation is highest at transformers in the South-East of New Zealand, near Dunedin ($\sim 0.5 \text{ A nT}^{-1} \text{ min}$), and some transformers near Christchurch ($\sim 0.2 \text{ A nT}^{-1} \text{ min}$). While we find a large hotspot in the South-East, we also find that the gradient can vary by a factor of two or more for transformers at the same location, that is, intra-substation variability, highlighting the importance of detailed modeling of the components of power infrastructure (e.g., Mac Manus, Rodger, Ingham, et al., 2022).

We then assess factors that could explain a portion of the scatter in the correlations, analyzing subsets of the SCs to test if sub-populations contain distinct behavior, as has been previously suggested in results from a single

location (Smith et al., 2022). First, we show that SCs that are followed by geomagnetic storms (i.e., SSCs) correspond to GICs that are on average 26% greater, compared to SIs, for the same per unit H' . Second, we show that SCs that occur when New Zealand is on the dayside of the Earth are linked to 27% greater GICs than if the SC occurs when New Zealand is on the nightside. Third, we find that SCs whose largest H' is oriented predominantly in the East-West direction are linked to 14% larger GICs, on average across New Zealand. These results highlight the importance of the vector direction and sub-minute resolution frequency content of the SC magnetic signature. Information on both is lost when the data are reduced to H' at a one minute cadence. Even for a relatively simple magnetic signature, this represents a source of scatter/uncertainty when mapping between the magnetic field and induced GICs.

Extrapolating our results to a reasonable but extreme event (for which $H' = 4000 \text{ nT min}^{-1}$), we find that most locations in New Zealand see maximum GIC below 500 A, while the Dunedin area would be exposed to a peak GIC of over 2000 A—an unprecedented level of GIC, well beyond any observations over the past 20 years.

Data Availability Statement

The results presented in this paper rely on the data collected at the Eyrewell magnetometer station. The data were downloaded from <https://intermagnet.github.io> and are freely available there. The New Zealand electrical transmission network DC measurements were provided to us by Transpower New Zealand with caveats and restrictions. This includes requirements of permission before all publications and presentations and no ability to provide the observations themselves. Requests for access to these characteristics and the DC measurements need to be made to Transpower New Zealand. At this time, the contact point is M. Dalzell (Michael.Dalzell@transpower.co.nz). The analysis in this paper was performed using python, including the pandas (McKinney, 2010), NumPy (Van Der Walt et al., 2011), SciPy (Virtanen et al., 2020), and Matplotlib (Hunter, 2007) libraries.

Acknowledgments

The authors thank the Institute of Geological and Nuclear Sciences Limited (GNS) for supporting its operation and INTERMAGNET for promoting high standards of magnetic observatory practice (www.intermagnet.org). AWS was supported by NERC Independent Research Fellowship NE/W009129/1. CJR and DHM were supported by the New Zealand Ministry of Business, Innovation, and Employment Endeavour Fund Research Programme contract UOOX2002. IJR is supported in part by STFC Grants ST/V006320/1 and ST/X001008/1, and NERC Grant NE/V002554/2. ARF was supported by Irish Research Council Government of Ireland Postdoctoral Fellowship GOIPD/2022/782. PAF acknowledges the support of a University of Otago Summer Research Scholarship.

References

- Akasofu, S.-I., & Chao, J. (1980). Interplanetary shock waves and magnetospheric substorms. *Planetary and Space Science*, 28(4), 381–385. [https://doi.org/10.1016/0032-0633\(80\)90042-2](https://doi.org/10.1016/0032-0633(80)90042-2)
- Araki, T. (1994). A physical model of the geomagnetic sudden commencement. In M. Engebretson, K. Takahashi, & M. Scholer (Eds.), *Solar wind sources of magnetospheric ultra-low-frequency waves* (p. 183).
- Bedrosian, P. A., & Love, J. J. (2015). Mapping geoelectric fields during magnetic storms: Synthetic analysis of empirical United States impedances. *Geophysical Research Letters*, 42(23), 10160–10170. <https://doi.org/10.1002/2015GL066636>
- Beggan, C. D. (2015). Sensitivity of geomagnetically induced currents to varying auroral electrojet and conductivity models. *Earth Planets and Space*, 67(1), 24. <https://doi.org/10.1186/s40623-014-0168-9>
- Beggan, C. D., Beamish, D., Richards, A., Kelly, G. S., & Alan, A. W. (2013). Prediction of extreme geomagnetically induced currents in the UK high-voltage network. *Space Weather*, 11(7), 407–419. <https://doi.org/10.1002/swe.20065>
- Beland, J., & Small, K. (2004). Space weather effects on power transmission systems: The cases of Hydro-Quebec and transpower New Zealand Ltd [Proceedings Paper]. In I. Daglis (Ed.), *Effects of space weather on technology infrastructure* (Vol. 176, pp. 287–299). Springer. PO BOX 17, 3300 AA.
- Blake, S. P., Gallagher, P. T., Campanyà, J., Hogg, C., Beggan, C. D., Thomson, A. W., et al. (2018). A detailed model of the Irish high voltage power network for simulating GICs. *Space Weather*, 16(11), 1770–1783. <https://doi.org/10.1029/2018SW001926>
- Blandin, M., Connor, H. K., Öztürk, D. S., Keesee, A. M., Pinto, V., Mahmud, M. S., et al. (2022). Multi-variate LSTM prediction of Alaska magnetometer chain utilizing a coupled model approach. *Frontiers in Astronomy and Space Sciences*, 9, 80. <https://doi.org/10.3389/fspas.2022.846291>
- Bolduc, L. (2002). GIC observations and studies in the Hydro-Québec power system. *Journal of Atmospheric and Solar-Terrestrial Physics*, 64(16), 1793–1802. [https://doi.org/10.1016/S1364-6826\(02\)00128-1](https://doi.org/10.1016/S1364-6826(02)00128-1)
- Boteler, D. H., Pirjola, R. J., & Nevanlinna, H. (1998). The effects of geomagnetic disturbances on electrical systems at the Earth's surface. *Advances in Space Research*, 22(1), 17–27. [https://doi.org/10.1016/S0273-1177\(97\)01096-X](https://doi.org/10.1016/S0273-1177(97)01096-X)
- Camporeale, E., Cash, M. D., Singer, H. J., Balch, C. C., Huang, Z., & Toth, G. (2020). A gray-box model for a probabilistic estimate of regional ground magnetic perturbations: Enhancing the NOAA operational Geospace model with machine learning. *Journal of Geophysical Research: Space Physics*, 125, (11), e2019JA027684. <https://doi.org/10.1029/2019JA027684>
- Cliilverd, M. A., Rodger, C. J., Brundell, J. B., Dalzell, M., Martin, I., Mac Manus, D. H., & Thomson, N. R. (2020). Geomagnetically induced currents and harmonic distortion: High time resolution case studies. *Space Weather*, 18(10). <https://doi.org/10.1029/2020SW002594>
- Cordell, D., Unsworth, M. J., Lee, B., Haneson, C., Milling, D. K., & Mann, I. R. (2021). Estimating the geoelectric field and electric power transmission line voltage during a geomagnetic storm in Alberta, Canada using measured magnetotelluric impedance data: The influence of three-dimensional electrical structures in the lithosphere. *Space Weather*, 19(10), e2021SW002803. <https://doi.org/10.1029/2021SW002803>
- Coughlan, M., Keesee, A., Pinto, V., Mukundan, R., Marchezi, J. P., Johnson, J., et al. (2023). Probabilistic forecasting of ground magnetic perturbation spikes at mid-latitude stations. *Space Weather*, 21(6), e2023SW003446. <https://doi.org/10.1029/2023SW003446>
- Dimitrakoudis, S., Milling, D. K., Kale, A., & Mann, I. R. (2022). Sensitivity of ground magnetometer array elements for GIC applications I: Resolving spatial scales with the BEAR and CARISMA arrays. *Space Weather*, 20(1), e2021SW002919. <https://doi.org/10.1029/2021SW002919>
- Dimmock, A. P., Rosenqvist, L., Hall, J. O., Viljanen, A., Yordanova, E., Honkonen, I., et al. (2019). The GIC and geomagnetic response over Fennoscandia to the 7–8 September 2017 geomagnetic storm. *Space Weather*, 17(7), 989–1010. <https://doi.org/10.1029/2018SW002132>

- Dimmock, A. P., Rosenqvist, L., Welling, D. T., Viljanen, A., Honkonen, I., Boynton, R. J., & Yordanova, E. (2020). On the regional variability of dB/dt and its significance to GIC. *Space Weather*, 18(8). <https://doi.org/10.1029/2020SW002497>
- Divett, T., Mac Manus, D. H., Richardson, G. S., Beggan, C. D., Rodger, C. J., Ingham, M., et al. (2020). Geomagnetically induced current model validation from New Zealand's South Island. *Space Weather*, 18(8). <https://doi.org/10.1029/2020SW002494>
- Divett, T., Richardson, G. S., Beggan, C. D., Rodger, C. J., Boteler, D. H., Ingham, M., et al. (2018). Transformer-level modeling of geomagnetically induced currents in New Zealand's South Island. *Space Weather*, 16(6), 718–735. <https://doi.org/10.1029/2018SW001814>
- Eastwood, J. P., Hapgood, M. A., Biffis, E., Benedetti, D., Bisi, M. M., Green, L., et al. (2018). Quantifying the economic value of space weather forecasting for power grids: An exploratory study. *Space Weather*, 16(12), 2052–2067. <https://doi.org/10.1029/2018SW002003>
- Fiori, R. A. D., Boteler, D. H., & Gillies, D. M. (2014). Assessment of GIC risk due to geomagnetic sudden commencements and identification of the current systems responsible. *Space Weather*, 12(1), 76–91. <https://doi.org/10.1002/2013SW000967>
- Fogg, A. R., Jackman, C. M., Coco, I., Rooney, L. D., Weigt, D. M., & Lester, M. (2023). Why are some solar wind pressure pulses followed by geomagnetic storms? *Journal of Geophysical Research: Space Physics*, 128(8), e2022JA031259. <https://doi.org/10.1029/2022JA031259>
- Fogg, A. R., Jackman, C. M., Malone-Leigh, J., Gallagher, P. T., Smith, A. W., Lester, M., et al. (2023). Extreme value analysis of ground magnetometer observations at Valentia observatory, Ireland. *Space Weather*, 21(7), e2023SW003565. <https://doi.org/10.1029/2023SW003565>
- Fogg, A. R., Lester, M., Yeoman, T. K., Carter, J. A., Milan, S. E., Sangha, H. K., et al. (2023). Multi-instrument observations of the effects of a solar wind pressure pulse on the high latitude ionosphere: A detailed case study of a geomagnetic sudden impulse. *Journal of Geophysical Research: Space Physics*, 128(3), e2022JA031136. <https://doi.org/10.1029/2022JA031136>
- Forsyth, C., Fazakerley, A. N., Rae, I. J., Watt, J., Murphy, K., Wild, J. A., et al. (2014). In situ spatiotemporal measurements of the detailed azimuthal substructure of the substorm current wedge. *Journal of Geophysical Research: Space Physics*, 119(2), 927–946. <https://doi.org/10.1002/2013JA019302>
- Friis-Christensen, E., McHenry, M. A., Clauer, C. R., & Vennerström, S. (1988). Ionospheric traveling convection vortices observed near the polar cleft: A triggered response to sudden changes in the solar wind. *Geophysical Research Letters*, 15(3), 253–256. <https://doi.org/10.1029/GL015i003p00253>
- Gaunt, C. T., & Coetzee, G. (2007). Transformer failures in regions incorrectly considered to have low GIC-risk. In *2007 IEEE Lausanne powertech, proceedings* (pp. 807–812). <https://doi.org/10.1109/PCT.2007.4538419>
- Gonzalez, W. D., Joselyn, J. A., Kamide, Y., Kroehl, H. W., Ros, G., Tsuru, B. T., & Vasyliunas, V. M. (1994). What is a geomagnetic storm? (Vol. 99). Tech. Rep. No. A4. <https://doi.org/10.1029/93JA02867>
- Hapgood, M., Angling, M. J., Attrill, G., Bisi, M., Cannon, P. S., Dyer, C., et al. (2021). Development of space weather reasonable worst-case scenarios for the UK national risk assessment. *Space Weather*, 19(4), e2020SW002593. <https://doi.org/10.1029/2020sw002593>
- Heyns, M. J., Lotz, S. I., & Gaunt, C. T. (2021). Geomagnetic pulsations driving geomagnetically induced currents. *Space Weather*, 19(2). <https://doi.org/10.1029/2020SW002557>
- Hunter, J. D. (2007). Matplotlib: A 2D graphics environment. *Computing in Science & Engineering*, 9(3), 90–95. <https://doi.org/10.1109/MCSE.2007.55>
- Keesee, A. M., Pinto, V., Coughlan, M., Lennox, C., Mahmud, M. S., & Connor, H. K. (2020). Comparison of deep learning techniques to model connections between solar wind and ground magnetic perturbations. *Frontiers in Astronomy and Space Sciences*, 7, 72. <https://doi.org/10.3389/fspas.2020.550874>
- Kokubun, S. (1983). Characteristics of storm sudden commencement at geostationary orbit. *Journal of Geophysical Research*, 88(A12), 10025–10033. <https://doi.org/10.1029/JA088iA12p10025>
- Love, J. J., Lucas, G. M., Rigler, E. J., Murphy, B. S., Kelbert, A., & Bedrosian, P. A. (2022). Mapping a magnetic superstorm: March 1989 geoelectric hazards and impacts on United States power systems. *Space Weather*, 20(5), e2021SW003030. <https://doi.org/10.1029/2021SW003030>
- Lühr, H., Schlegel, K., Araki, T., Rother, M., & Förster, M. (2009). Night-time sudden commencements observed by CHAMP and ground-based magnetometers and their relationship to solar wind parameters. *Annales Geophysicae*, 27(5), 1897–1907. <https://doi.org/10.5194/angeo-27-1897-2009>
- Mac Manus, D. H., Rodger, C. J., Dalzell, M., Renton, A., Richardson, G. S., Petersen, T., & Clilverd, M. A. (2022). Geomagnetically induced current modeling in New Zealand: Extreme storm analysis using multiple disturbance scenarios and industry provided hazard magnitudes. *Space Weather*, 20(12), e2022SW003320. <https://doi.org/10.1029/2022SW003320>
- Mac Manus, D. H., Rodger, C. J., Dalzell, M., Thomson, A. W. P., Clilverd, M. A., Petersen, T., et al. (2017). Long-term geomagnetically induced current observations in New Zealand: Earth return corrections and geomagnetic field driver. *Space Weather*, 15(8), 1020–1038. <https://doi.org/10.1002/2017SW001635>
- Madsen, F. D., Beggan, C. D., & Whaler, K. A. (2022). Forecasting changes of the magnetic field in the United Kingdom from L1 Lagrange solar wind measurements. *Frontiers in Physics*, 0, 1091. <https://doi.org/10.3389/fphy.2022.1017781>
- Mayaud, P. N. (1973). *A hundred year series of geomagnetic data, 1868–1967: Indices aa, storm sudden commencements(SSC)* (p. 256). IUGG Publ. Office.
- McKinney, W. (2010). Data structures for statistical computing in python. Retrieved from <http://conference.scipy.org/proceedings/scipy2010/mckinney.html>
- Moretto, T., Friis-Christensen, E., Lühr, H., & Zesta, E. (1997). Global perspective of ionospheric traveling convection vortices: Case studies of two Geospace Environmental Modeling events. *Journal of Geophysical Research*, 102(A6), 11597–11610. <https://doi.org/10.1029/97JA00324>
- Ngwira, C. M., Pulkkinen, A. A., Bernabeu, E., Eichner, J., Viljanen, A., & Crowley, G. (2015). Characteristics of extreme geoelectric fields and their possible causes: Localized peak enhancements. *Geophysical Research Letters*, 42(17), 6916–6921. <https://doi.org/10.1002/2015GL065061>
- Ngwira, C. M., Sibeck, D., Silveira, M. V. D., Georgiou, M., Weygand, J. M., Nishimura, Y., & Hampton, D. (2018). A study of intense local dB/dt variations during two geomagnetic storms. *Space Weather*, 16(6), 676–693. <https://doi.org/10.1029/2018SW001911>
- Oliveira, D. M., Arel, D., Raeder, J., Zesta, E., Ngwira, C. M., Carter, B. A., et al. (2018). Geomagnetically induced currents caused by interplanetary shocks with different impact angles and speeds. *Space Weather*, 16(6), 636–647. <https://doi.org/10.1029/2018SW001880>
- Oughton, E. J., Hapgood, M., Richardson, G. S., Beggan, C. D., Thomson, A. W., Gibbs, M., et al. (2019). A risk assessment framework for the socioeconomic impacts of electricity transmission infrastructure failure due to space weather: An application to the United Kingdom. *Risk Analysis*, 39(5), 1022–1043. <https://doi.org/10.1111/risa.13229>
- Pinto, V. A., Keesee, A. M., Coughlan, M., Mukundan, R., Johnson, J. W., Ngwira, C. M., & Connor, H. K. (2022). Revisiting the ground magnetic field perturbations challenge: A machine learning perspective. *Frontiers in Astronomy and Space Sciences*, 9, 123. <https://doi.org/10.3389/fspas.2022.869740>
- Pulkkinen, A., Lindahl, S., Viljanen, A., & Pirjola, R. (2005). Geomagnetic storm of 2931 October 2003: Geomagnetically induced currents and their relation to problems in the Swedish high-voltage power transmission system. *Space Weather*, 3(8). <https://doi.org/10.1029/2004SW000123>

- Pulkkinen, A., Rastätter, L., Kuznetsova, M., Singer, H., Balch, C., Weimer, D., et al. (2013). Community-wide validation of geospace model ground magnetic field perturbation predictions to support model transition to operations. *Space Weather*, *11*(6), 369–385. <https://doi.org/10.1002/swe.20056>
- Pulkkinen, A., Thomson, A., Clarke, E., & McKay, A. (2003). April 2000 geomagnetic storm: Ionospheric drivers of large geomagnetically induced currents. *Annales Geophysicae*, *21*(3), 709–717. <https://doi.org/10.5194/angeo-21-709-2003>
- Rajput, V. N., Boteler, D. H., Rana, N., Saiyed, M., Anjana, S., & Shah, M. (2020). Insight into impact of geomagnetically induced currents on power systems: Overview, challenges and mitigation. *Electric Power Systems Research*, *192*, 106927. <https://doi.org/10.1016/J.EPSR.2020.106927>
- Rodger, C. J., Clilverd, M. A., Mac Manus, D. H., Martin, I., Dalzell, M., Brundell, J. B., et al. (2020). Geomagnetically induced currents and harmonic distortion: Storm-time observations from New Zealand. *Space Weather*, *18*(3), e2019SW002387. <https://doi.org/10.1029/2019SW002387>
- Rodger, C. J., Mac Manus, D. H., Dalzell, M., Thomson, A. W. P., Clarke, E., Petersen, T., et al. (2017). Long-term geomagnetically induced current observations from New Zealand: Peak current estimates for extreme geomagnetic storms. *Space Weather*, *15*(11), 1447–1460. <https://doi.org/10.1002/2017SW001691>
- Rogers, N. C., Wild, J. A., Eastoe, E. F., Gjerloev, J. W., & Thomson, A. W. P. (2020). A global climatological model of extreme geomagnetic field fluctuations. *Journal of Space Weather and Space Climate*, *10*, 5. <https://doi.org/10.1051/swsc/2020008>
- Russell, C. T., Ginskey, M., Petrinec, S., & Le, G. (1992). The effect of solar wind dynamic pressure changes on low and mid-latitude magnetic records. *Geophysical Research Letters*, *19*(12), 1227–1230. <https://doi.org/10.1029/92GL01161>
- Smith, A. W., Forsyth, C., Rae, I. J., Garton, T. M., Bloch, T., Jackman, C. M., & Bakrania, M. (2021). Forecasting the probability of large rates of change of the geomagnetic field in the UK: Timescales, horizons and thresholds. *Space Weather*, e2021SW002788. <https://doi.org/10.1029/2021SW002788>
- Smith, A. W., Forsyth, C., Rae, J., Rodger, C. J., & Freeman, M. P. (2021). The impact of sudden commencements on ground magnetic field variability: Immediate and delayed consequences. *Space Weather*, *19*(7), e2021SW002764. <https://doi.org/10.1029/2021SW002764>
- Smith, A. W., Freeman, M. P., Rae, I. J., & Forsyth, C. (2019). The influence of sudden commencements on the rate of change of the surface horizontal magnetic field in the United Kingdom. *Space Weather*, *17*(11), 1605–1617. <https://doi.org/10.1029/2019SW002281>
- Smith, A. W., Rae, I. J., Forsyth, C., Oliveira, D. M., Freeman, M. P., & Jackson, D. R. (2020). Probabilistic forecasts of storm sudden commencements from interplanetary shocks using machine learning. *Space Weather*, *18*(11). <https://doi.org/10.1029/2020SW002603>
- Smith, A. W., Rodger, C. J., Mac Manus, D. H., Forsyth, C., Rae, I. J., Freeman, M. P., et al. (2022). The correspondence between sudden commencements and geomagnetically induced currents: Insights from New Zealand. *Space Weather*, *20*(8), e2021SW002983. <https://doi.org/10.1029/2021SW002983>
- Southwood, D. J., & Kivelson, M. G. (1990). The magnetohydrodynamic response of the magnetospheric cavity to changes in solar wind pressure. *Journal of Geophysical Research*, *95*(A3), 2301–2309. <https://doi.org/10.1029/JA095iA03p02301>
- Takeuchi, T., Araki, T., Viljanen, A., & Watermann, J. (2002). Geomagnetic negative sudden impulses: Interplanetary causes and polarization distribution. *Journal of Geophysical Research*, *107*(A7), 1096. <https://doi.org/10.1029/2001JA900152>
- Thomson, A. W., Dawson, E. B., & Reay, S. J. (2011). Quantifying extreme behavior in geomagnetic activity. *Space Weather*, *9*(10). <https://doi.org/10.1029/2011SW000696>
- Upendran, V., Tigas, P., Ferdousi, B., Bloch, T., Cheung, M. C. M., Ganju, S., et al. (2022). Global geomagnetic perturbation forecasting using Deep Learning. *Space Weather*, *20*(6), e2022SW003045. <https://doi.org/10.1029/2022SW003045>
- Van Der Walt, S., Colbert, S. C., & Varoquaux, G. (2011). The NumPy array: A structure for efficient numerical computation. *Computing in Science & Engineering*, *13*(2), 22–30. <https://doi.org/10.1109/MCSE.2011.37>
- Viljanen, A., Nevanlinna, H., Pajunpää, K., & Pulkkinen, A. (2001). Time derivative of the horizontal geomagnetic field as an activity indicator. *Annales Geophysicae*, *19*(9), 1107–1118. <https://doi.org/10.5194/angeo-19-1107-2001>
- Virtanen, P., Gommers, R., Oliphant, T. E., Haberland, M., Reddy, T., Cournapeau, D., et al. (2020). SciPy 1.0: Fundamental algorithms for scientific computing in Python. *Nature Methods*, *17*(3), 261–272. <https://doi.org/10.1038/s41592-019-0686-2>
- Wintoft, P., Wik, M., & Viljanen, A. (2015). Solar wind driven empirical forecast models of the time derivative of the ground magnetic field. *Journal of Space Weather and Space Climate*, *5*, A7. <https://doi.org/10.1051/swsc/2015008>
- Yue, C., Zong, Q. G., Zhang, H., Wang, Y. F., Yuan, C. J., Pu, Z. Y., et al. (2010). Geomagnetic activity triggered by interplanetary shocks. *Journal of Geophysical Research*, *115*(A5), A00I05. <https://doi.org/10.1029/2010JA015356>
- Zhou, X., & Tsurutani, B. T. (2001). Interplanetary shock triggering of nightside geomagnetic activity: Substorms, pseudobreakups, and quietest events. *Journal of Geophysical Research*, *106*(A9), 18957–18967. <https://doi.org/10.1029/2000JA003028>